STRUCTURE DEVELOPMENT FROM SIMULTANEOUS PHASE SEPARATION AND CRYSTALLIZATION OF METALLOCENE POLYOLEFIN BLENDS

Charles C. Han, Howard Wang, Katsumi Shimizu, Hongdoo Kim, Erik Hobbie, Zhi-Gang Wang

Polymers Division, National Institute of Standards and Technology
Gaithersburg, MD 20899

Introduction

Olefin polymers are the most widely used materials in the plastics industry today. To optimize their properties and processibility, blending is often used[1]. This is particularly important for the metallocene-catalyst based polyolefins. By altering certain shear-thinning and strain-hardening characteristics, blending can enhance the processibility of the material. This is in addition to any property enhancement or modification already formulated into the blending or alloying process. In the case of polyolefin blends, the mixtures can undergo both liquid-liquid phase separation (LLPS) and crystallization, complicating the blend morphology[2]. This complication can be either advantageous or disadvantageous in term of structural control/property tailoring, depending on whether or not complex structures yield desired properties of the final product. To fully understand and utilize the potential of the complex morphology arising from LLPS and crystallization under non-equilibrium processing conditions such as shear and temperature gradient, we carried out a systematic study involving both multi-scale characterization and multi-scale computer modeling on a model polyolefin blend. Comprehensive measurements of the morphology and rheology of the blend as a function of composition, temperature, pressure, shear rate, phase miscibility, crystalline structure, and thermal history are being carried out to form constitutive relationships that can be used for the input of computer modeling for pre-product evaluation, performance prediction and process design etc.

In this study, we investigated the dynamics of structure evolution in polyolefin blends undergoing simultaneous LLPS and crystallization or cyclic crystallization and melting (CCM) after LLPS. In the former case, by controlling relative quench depths for LLPS and crystallization, the growth kinetics of the characteristic length shows a crossover of linear dynamics from crystallization to LLPS, separated by a non-linear regime where both ordering processes are important. In the latter, CCM enhances large-scale domain coarsening while introducing fine structures within domains.

Experimental

The statistical copolymers of ethylene/hexene (PEH) and ethylene/butene (PEB) were obtained from ExxonMobil Inc.,[4] and were both synthesized using metallocene catalysts. The characteristics of the two polymers, including weight averaged molecular mass (M_w), mass density (ρ_m), branching density [ρ_b, in unit of per 1000 backbone carbon atoms (kC)] as well as the equilibrium melting temperature (T_m^o) are listed in Table 1. The melting temperature of PEB, ca. 40 °C, was measured by a single differential scanning calorimetry scan with a scan rate of 10 °C/min. In the scope of this study, PEB can be considered as an essentially amorphous component.

Table 1. Characteristics of PEH, PEB and Their Blend.

	M_w (kg/mol)	ρ_m(g/cm^3)	ρ_b(kC^{-1})	T_m^o (°C)
PEH	110	0.922	18	141
PEB	70	0.875	77	--

Because of the almost identical refractive index and slow kinetics, the phase boundary (temperature/composition) of LLPS has been determined using crystallization induced contrast technique[3]. The PEH/PEB blend has an upper critical solution temperature of 146 °C in the melt region. The composition dependence of the LLPS boundary follows the prediction of Flory-Huggins theory for binary polymer mixtures. T_m^o of the blends decreases from 141 ± 3 °C for pure PEH with increasing PEB concentration in the miscible phase, whereas it remains relatively constant at 127 ± 3 °C within the LLPS coexistence region. (Fig. 1)

The blends were prepared by co-precipitating from a hot (*ca*. 100 °C) common xylene solution into cold methanol. After filtering, the polymers were dried in air for a day, and further dried in vacuum oven at 100 °C for 3 days. The mixtures were hot-pressed between a glass slide and a glass cover at 160 °C to films of 20 to 30 μm. For phase contrast optical microscopy studies, blends with equal mass fraction of PEH and PEB (denoted as H50) were kept in the melt at 160 °C for 5 min and then quickly cooled down to the isothermal temperatures, T_c. Crystallization and LLPS morphology was recorded at various times, and their characteristic lengths were measured from images. In the CCM study, a blend with 60 % mass fraction of PEH (denoted as H60) was first isothermally annealed at 130 °C for 240 min, followed by alternating crystallization at 110 °C and re-melting at 130 °C. The morphology was recorded at each stage. The variation for the isothermal temperature was within ± 0.2 °C.

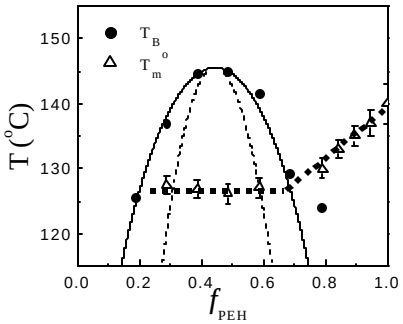

Figure 1. Phase diagram of the PEH/PEB blend. The solid circles and the open triangles are measured values of liquid-liquid phase separation temperatures and the equilibrium melting temperature, T_m^o, respectively. The solid and dashed curves are calculated binodal and spinodal boundaries, respectively, and the dotted line is to guide to the eye. The phase diagram shows an upper critical solution temperature, $T_{s,c}$ = 146 °C, and f_c = 0.44.

Results and Discussion

Figure 2 shows optical micrographs of the blend after isothermal storage for (a) 64 min at 112 °C, (b) 960 min at 115 °C, and (c) 1200 min at 121 °C, and subsequently quenched to room temperature. Figure 2a shows that spherulites grow and impinge upon each other, with crystallization being the dominant phase-ordering process. The light sheaf-like features in Fig. 2b are early-stage spherulites that grow mostly during the first 60 min of the isothermal annealing. At a later time, crystal growth at that temperature is suppressed. Morphological change is mostly limited to the matrix region. After 1200 min at 121 °C, small crystals are sparsely distributed within the sample. Upon quenching to room temperature, the bicontinuous morphology due to LLPS becomes evident (Fig. 2c).

This nonlinear morphology development dynamic is understood by examining the driving force for structural evolution. For large under-cooling, T_c = 112 °C, crystallization clearly dominates the morphological development. For T_c = 115 °C, crystallization is prominent at the early times when the blend is relatively homogeneous in composition. As the crystals grow, liquid-liquid phase separation proceeds in the matrix, resulting in a composition variation that is larger in both wavelength and amplitude. The high barrier of the depleted region due to composition inhomogeneity prohibits baby spherulites from maturing into spherical shapes. Further crystallization is confined within phase-separated, bi-continuous tubes. At small undercooling, T_c = 121 °C, crystallization proceeds very slowly, and the growth of phase-separated domains is the faster process. Crystallization is thus mainly confined to the already established liquid-liquid separated domains. After quenching to room temperature, the crystallizable component in both of the co-existing liquid phases crystallizes, resulting in markedly different refractive indices and significant optical contrast between the two phases.

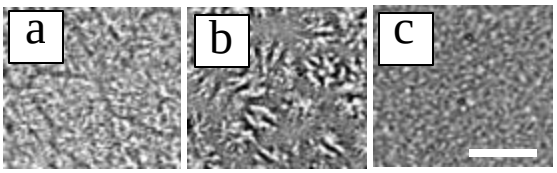

Figure 2. Optical micrographs of the H50 blend after annealing for (a) 64 min at 112 °C, (b) 960 min at 115 °C, and (c) 1200 min at 121 °C, and subsequently quenched to room temperature. The scale bar represents 20 μm.

As an approximation, LLPS and crystallization can be considered as independent processes for isothermal temperatures above and far below the T_m^o of H50. In this study, the relevant LLPS process is the late-stage spinodal decomposition, where hydrodynamic forces drive the coarsening, and the phase-coarsening kinetics follows the simple growth law[5]

$$l \propto \frac{s}{h} t \quad (1)$$

where s and h are the interfacial tension between the co-existing phases and effective viscosity of the fluid, respectively, and t is the time following a quench into the unstable region of the phase diagram. Following a scaling argument for late-stage LLPS, the growth rate of the characteristic length is found depending on the reduced-temperature quench depth for LLPS,

$$l/t \sim (T_s - T)/T_s, \quad (2)$$

On the other hand, the crystal growth rate depends on the crystallization mechanism. In regime I, single crystal nucleation at a crystal surface causes layer-by-layer growth, whereas in regime II, because of the large secondary nucleation rate at high under-cooling, multiple nuclei exist on the same crystallization surface. A unified formalism gives the growth rate as

$$G_i = k_i e^{Q_D^*/RT_c} e^{-K_{g,i}/(T_c^* \Delta T)}, \quad (3)$$

where the subscript i denotes I or II (for regime I or II), ΔT is the difference between T_m^o and T_c, k and R are molecular and thermal constants, respectively, Q_D^* is the activation energy for steady-state reptation, and K_g is the nucleation constant[6].

Based on these arguments, the growth rates of the two ordering processes are shown in Fig. 3. The solid and dashed lines depict the rate of crystal superstructure growth and phase coarsening, respectively. The crystallization growth rate is the measured value, while the growth rate for phase separation is estimated from the scaling law described above, with the coefficient of proportionality given by fitting the measured l(t) at 130 °C, as shown in the inset. This argument of independent linear dynamics of LLPS and crystallization provides rather accurate pictures of structural dynamics at high and low temperatures, respectively, where the interplay between the two is not significant. In the crossover regime, however, complex structures can form due to the interference between LLPS and crystallization (Fig. 2b).

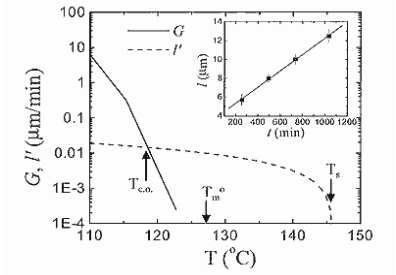

Figure 3. A comparison of growth rates for LLPS and crystallization as a function of isothermal temperature.

In CCM study, the effect of crystal growth on the melt transport dynamic is examined. Figure 4 shows the melt morphology of H60 at 130 °C (a) before and after (b) 1, (c) 2 and (d) 4 cycles of crystallization at 110 °C and remelting at 130 °C. Fig. 4a shows that LLPS morphology is barely discernible after 240 min at 130 °C, implying both small feature size (slow kinetics) and little difference in refractive indices of the coexisting liquid phases. After one CCM, domains of *ca*. 30 μm are visible (Fig. 4b). With additional cycles, the feature size remains relatively constant, whereas the contrast increases (Figs. 4c and d). This nonlinear dynamics is due to the interplay between crystal growth and melt transport. Following a second quench after LLPS, crystals grow predominantly in PEH-rich phase, garnering crystallizable PEH chains and expelling PEB chains. This process changes the composition in the melt and enhances the coarsening of PEB-rich domains. The details of the domain structure are elucidated in Fig. 5. The crystalline structure of the blend after 3.5 cycles (Fig. 5a) is compared to its subsequent melt morphology (Fig. 5b). The lighter regions in Fig.5a represent crystalline phase, corresponding to the darker regions (PEH-rich) in Fig. 5b. It is clear that in addition to large-scale structures, fine structures of a few microns exist in both semi-crystalline and molten states. They represent entities of super structure crystallites in the former and concentrated PEH melt in the latter.

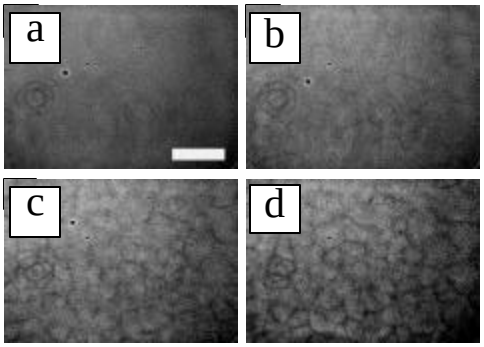

Figure 4. The melt morphology of H60 at 130 °C (a) before and after (b) 1, (c) 2 and (d) 4 cycles of crystallization at 110 °C and re-melting at 130 °C. The scale bar represents 50 μm.

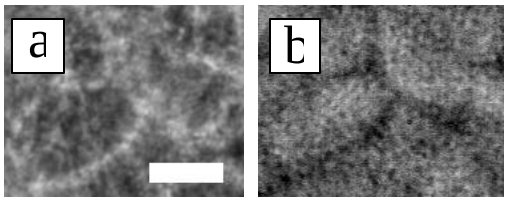

Figure 5. A comparison between the (a) crystalline and (b) melt morphology in the same area after CCM. The scale bar represents 20 μm.

Nonlinear dynamics of structural formation is often driven by high order non-equilibrium free energy density. During the first CCM process, the balance of equilibrium chemical potentials between coexisting liquid phases is broken, and non-equilibrium potentials due to the quenched degree of freedoms and trapped chemical inhomogeneity prevail. Crystal growth causes hydrodynamic interaction and rapid coarsening in the melt. This effect is significant only when the length-scale of the crystal super structure is comparable to the scale of the composition modulation in the melt. With increasing cycles of CCM, scale mismatch leads to little further change of large-scale domain structure, however, continued local segregation and deepening compositional trap enhances the optical contrast.

Conclusion

Non-linear structural dynamics in polymer blends can be expected when dual or multiple phase ordering processes co-exist. In a typical case of LLPS and crystallization co-existence in polyolefin blends, linear dynamics of crystal growth and LLPS is observed at low and high temperatures respectively, where interferences from each other is negligible. In the cross-over regime, interplay between LLPS and crystallization causes non-linear ordering because of the structural and rheological heterogeneity. On the other hand, cyclic crystallization and melting in a previously phase-separated blend causes immediate large-scale coarsening and progressive fine-scale sharpening. In view of the obvious importance to many applications, the potential of complex structures arising from non-linear dynamics in polymer blends need much in-depth exploration.

Acknowledgement We acknowledge Dr. David J. Lohse for providing material for this study and Dr. Freddy A. Khoury for insightful discussion.

References

(1) Paul, D. R.; Bucknall, C. B., *Polymer Blends*, John Wiley and Sons, Inc., New York, **2000**.
(2) Crist, B.; Hill, M. J., *J Polym. Sci.: Polym. Phys.*, **1997**, *35*, 2329.
(3) Wang H, et al., *Macromolecules* **2002**, *35*, 1072.
(4) The references to commercial equipment or materials do not imply recommendation or endorsement by the National Institute of Standards and Technology.
(5) E. D. Siggia, Phys. Rev. A. **1979,** *20*, 595.
(6) J. D. Hoffman, G. T. Davis, and J. I. Laurizten, in *Treatise on Solid State Chemistry, V3; Crystalline and Non-crystalline Solids*, N. B. Hannay Ed., Plenum, New York, **1976**.